Synthesis of Iron Oxide Nanoparticles to Enhance Polysulfone Ultrafiltration Membrane performance for Salt Rejection

Muneer M. Ba-Abbad*[a,b,d], Abdul Wahab Mohammad[a,b], Mohd S. Takriff[a,b], Rosiah Rohani[a,b], Ebrahim Mahmoudi[a,b], Khalefa A. Faneer[a,b], Abdelbaki Benamo[c]

[a]Department of Chemical and Process Engineering, Faculty of Engineering and Built Environment, Universiti Kebangsaan Malaysia, 43600, Bangi, Selangor, Malaysia.
[b]Research Centre for Sustainable Process Technology (CESPRO), Faculty of Engineering and Built Environment, Universiti Kebangsaan Malaysia, 43600, Bangi, Selangor, Malaysia.
[c]Gas Processing Centre, Qatar University, P. O. Box 2713 Doha, Qatar.
[d]Department of Chemical Engineering, Faculty of Engineering and Petroleum, Hadhramout University of Science &Technology,
Mukalla, Hadhramout, Yemen.
muneer711@gmail.com

The main target of membrane technologies is to provide better filtration and separation of organic and inorganic substance from water as well as for longer life of the membrane. Iron oxide (α-Fe_2O_3) nanoparticles (NPs) were synthesised by simple sol gel method and characterised using X-ray diffraction (XRD) and transmission electron microscopy (TEM) to show the structure and particle size of the nanoparticles. The α-Fe_2O_3 NPs with the size of 15 ± 2 nm was blended with Polysulfone (PSf) in lower loading of 0.5 wt% to prepare ultrafiltration (UF) membrane using the wet phase inversion method. The membrane cross section, surface, EDX and mapping were analysed using field emission scanning electron microscopy (FESEM) include EDX analyser. The effect of α-Fe_2O_3 NPs on membrane properties was determined in terms of permeability, hydrophilicity (contact angle), porosity and pore size. The results of α-Fe_2O_3 NPs incorporated PSf showed good improvement in the hydrophilicity of the membrane where the contact angle was reduced from 82° to 70°. The pure water flux of α-Fe_2O_3 NPs-incorporated PSf membrane increased to more than three times compared to the pure PSf membrane. This enhancement of pure flux was due to lower intrinsic membrane resistance and higher pore size. The rejection of salts (sodium chloride (NaCl) and sodium sulfate (Na_2SO_4)) of the modified membrane was enhanced compared to pure PSf membrane under the same condition. The addition of α-Fe_2O_3 NPs leads to an improvement of the PSf ultrafiltration membrane properties.

1. Introduction

Ultrafiltration (UF) membranes have been increasingly used for wide applications in water and wastewater treatment, food and biotechnology industries. The main disadvantage of UF membranes during filtration is fouling (Luo et al. 2005). Different types of fouling have been reported in membrane system such as organic fouling, particulate and microbial fouling (Chung et al., 2016). There are several ways that can be used to reduce and control the membrane fouling namely (i) pretreatment of the feed solution,(ii) modification of the membrane surface and (iii) control conditions and periodic cleaning of the process (Mahmoudi et al., 2015).
Polymer such as Polysulfone (PSf) has been used for fabricating microfiltration, ultrafiltration and nanofiltration membranes due to the good chemical and thermal resistance properties and ease of processing (Boussu et al., 2006). The PSf is a hydrophobic material, making its surface prone to fouling which affects its application and usage life (Luo et al., 2005). Recently, many researches have focused on reducing the membrane fouling by adding nanoparticles to increase the hydrophilicity (Chung et al., 2015). These studies can be divided into three categories: (1) blending PSF with hydrophilic nanoparticles, (2) grafting with hydrophilic polymers, (3)

adding monomers or functional groups and coating with hydrophilic polymers (Ba-Abbad et al., 2012). The blending of metal oxide nanoparticles with membrane has resulted in an improvement of the membrane properties, such as the contact angle, flux, etc. (Ba-Abbad et al., 2015). This work focused on the improvement of UF membrane performance by blending with iron oxide nanoparticles. Both membranes were characterised to investigate their contact angle, flux and structure. The blended membrane was used for salt rejection and compared to pure PSf membrane performance.

2. Experimental Methods

2.1 Materials

For the synthesis of iron oxide nanoparticles (α-Fe$_2$O$_3$), the iron nitrate was supplied by BDH Prolabo Chemicals, UK. The ethanol and oxalic acid were ordered form R&M Chemicals Company. The PSf pellet was used as the main polymer for the membrane together with solvent N-Methyl-2-pyrrolidone (NMP). Both were received form Sigma Company. Sodium chloride and sodium sulphate salts were obtained from R&M Chemicals Company.

2.2 Synthesis of iron oxide nanoparticles (α-Fe$_2$O$_3$ NP)

The sol-gel method was used to prepare α-Fe$_2$O$_3$ NP under low temperature of refluxing. The optimum values of all reactants as molar ratio between the iron nitrate and oxalic acid were 1 : 2 under pH of 2.0 ± 0.2 and calcination temperature of 400 °C as reported in our previous study to produce smaller size of NP (Ba-Abbad et al., 2013a; 2013b).

2.3 Preparation of membrane

Pure PSf and blend PSf membranes with α-Fe$_2$O$_3$ NP were prepared by wet phase inversion method. The lower concentrations of α-Fe$_2$O$_3$ NP of 0.5 wt% were applied to avoid the agglomeration of NP within the blending process (without adding of copolymer) because of the magnetic properties of α-Fe$_2$O$_3$ NP. About 18 % of PSf was mixed with N-Methyl-2-pyrrolidone (NMP) 82 % under mechanical stirring overnight at 200 rpm until completely dissolved. For modified membrane, 0.5 wt% were mixed with previous solution for 1 h and sonicated it for 10 min then continues with stirring for another 1 h. The final solution was left for 3 h for degassing before casting. The membranes were cast by a Filmographe doctor blade 360099003 (Braive Instrument, Germany) with 0.2 mm thickness at room temperature. After casting, the membranes were immersed in water bath overnight before being used and characterised.

2.4 Characterisations of α-Fe$_2$O$_3$ NP and membrane

The α-Fe$_2$O$_3$ NP was investigated for their size and structure phase using X-ray diffractometer (XRD) (Bruker D8 Advance AXS X-ray diffractometer), with 2θ scanning between 20 °C to 80 °C using Cu-Kα radiation (1.5406 Å) and the Debye–Scherer equation. The shape and size of α-Fe$_2$O$_3$ NP were imaged by the Transmission Electron Microscope (TEM) (Philips CM200, model JEOLJEM 2100). The contact angle (membrane hydrophilicity) was evaluated using Kruss Easy Drop with DROP image Standard Software and ultrapure water room temperature as the media. The surface and cross section of the fabricated membranes were viewed by the Field Emission Scanning Electron Microscope (FESEM) (SUPRA 55VP). The element and mapping were measured by energy-dispersive X-ray spectroscopy (EDX) (Oxford EDX INCA Penta FETX3). The rejection performance of the fabricated membranes was investigated by measuring conductivity of salt before and after filtration using Mettler Toledo's conductivity meter.

2.5 Membrane performance

The performance of the PSf and modified PSf as UF membranes was investigated by measuring the permeate flux and rejection. The permeate flux were evaluated by Eq(1):

$$J = \frac{V}{A.t}$$ (1)

Where J is the measured permeate flux (L/m^2 h), V is the accumulative of permeate volume (L), t = is the time of filtration (h), A is the effective area of the fabricated membrane (m^2)

The salt rejection was evaluated using the 20 mg/L as initial salt concentration under 3 bar during the filtration process using the Eq(2):

$$R = 1 - \frac{C_p}{C_f} \times 100$$ (2)

Where R is rejection, C_p is the permeate concentration (mg/L), C_f is the feed concentration (mg/L)

3. Results and discussions

3.1 Crystal structure and morphology of synthesised α-Fe₂O₃ NP

The crystal structure and size of α-Fe_2O_3 NP was determined by using X-ray diffraction (XRD). The structure of rhombohedral hematite with lattice parameters of a = 0.503560 nm and b = 1.37489 nm was obtained which matched with JCPDS 033-0664. All the peaks of XRD pattern was found to match with JCPDS 033-0664 of α-Fe_2O_3 NP as shown in Figure 1(a). The crystal size was calculated using Bragg's and Scherrer's equation and was found to be 17 ± 2 nm.

Figure 1: Characterisation of α-Fe2O3 NP (a) XRD, (b) TEM

The morphology of synthesised α-Fe_2O_3 NP was viewed by transmission electron microscope (TEM). The spherical shape of α-Fe_2O_3 NP with slight agglomeration was observed and can be attributed to the magnetic properties of NP. The average particle size was found to be 18 ± 2 nm which showed good agreement with the XRD results.

3.2 Characterisation of the membranes

Generally, the contact angle indicates the degree of surface hydrophilicity of the membrane. The pure water flux and contact angles of PSf and modified PSf membranes were measured at room temperature. The contact angle of the modified PSf was reduced if compared to the pure PSf as shown in Figure 2. The contact angle was reduced from 82.7° ± 0.90° to 70.1° ± 2.55° which can be attributed to the reduced interface energy of the mixed matrix membranes caused by the functional groups of α-Fe_2O_3 NP on the surface of the PSf membrane (Vatanpour et al., 2011). However, the water flux of the membranes showed direct influence by the hydrophilicity improvement. Higher water flux by the modified PSf (0.5 wt%) was observed when compared to the pure PSf membrane. By increasing the amount of α-Fe_2O_3 NP up to 1.0 wt%, the flux was decreased due to the increase of the blend solution viscosity which delays the mass transfer between the solvent and non-solvent phase (Ba-Abbad et al., 2016).
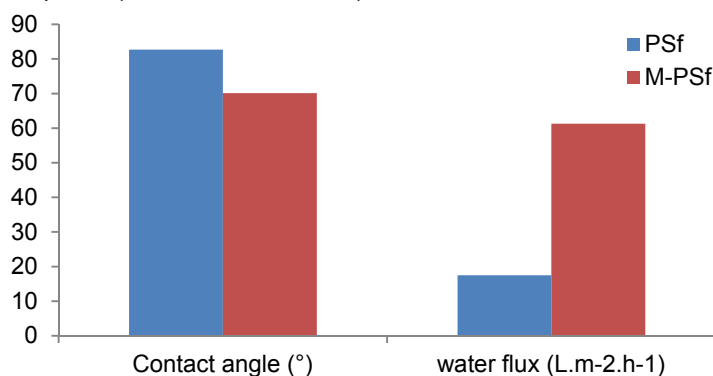
Figure 2: Contact angle and pure water flux at 4 bar of the PSf and modified PSf membranes (0.5 wt%)

Figure 3 showed the surface and cross-sectional images of the PSf and modified PSf membranes which were obtained using FESEM. The surface of the modified PSf membrane is smooth with no α-Fe$_2$O$_3$ NP or agglomerations on the top surface compared to the pure PSf (Figure 3(b)). This result was attributed to the fact that α-Fe$_2$O$_3$ NP had incorporated well with the PSf matrix, leading to an improvement of their properties. The cross-sectional images of PSf and modified PSf membranes are shown in Figure 3(a1) and (b1). From these results, it was observed that the membrane structure has a typical asymmetric morphology with finger-like pores linked by sponge walls.
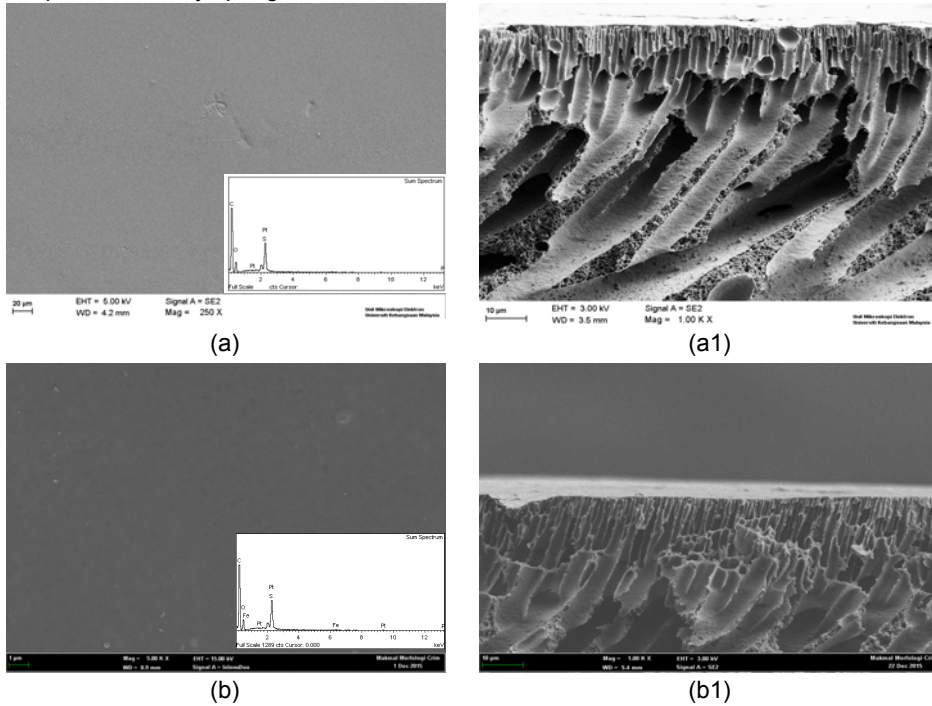

(a)

(a1)

(b)

(b1)

Figure 3: Surface and cross-sectional SEM images of the prepared membranes with EDX spectrum: (a, a1) Pure PSf and (b, b1) modified PSf membranes (0.5 wt.%)

In order to investigate how well the α-Fe$_2$O$_3$ NP was incorporated into the PSF matrix, the EDX analysis was applied. All peaks of α-Fe$_2$O$_3$ NP appeared after blending with PSf compared to pure PSf, which was attributed to the presence of α-Fe$_2$O$_3$ NP in membrane. The mapping of α-Fe$_2$O$_3$ NP distribution was evaluated and given in Figure 4. Uniform distribution of α-Fe$_2$O$_3$ NP in PSf membrane matrix was obtained which was attributed to a very good preparation of α-Fe$_2$O$_3$ NP by sol gel method and blending with the PSf solution (Ba-Abba et al., 2013c).
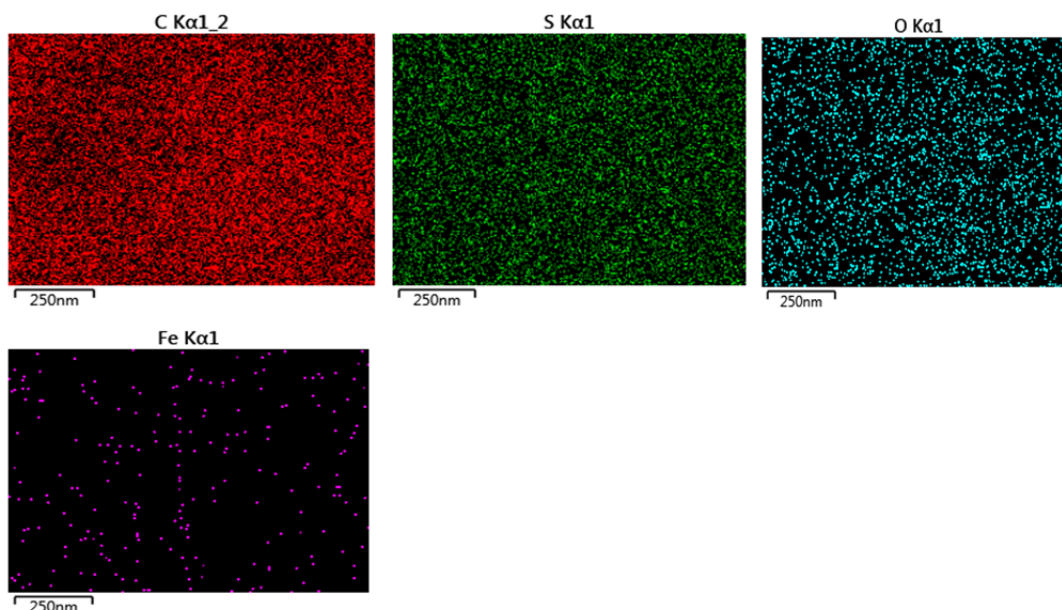
Figure 4: Mapping of blend α-Fe2O3 NP with PSf membrane

3.3 Performance of the membranes

Figure 5 shows the results of salt rejection of PSf and modified PSf membranes. The rejection for PSf and modified PSf membranes were 44 % and 47 % for monovalent of sodium chloride as well as 50 % and 54 % for divalent sodium sulphate. Based on the salt rejection, the modified membrane exhibited slightly higher rejection than pure PSf. The reason for this increase was due to slight enhancement of the hydrophilicity of the modified PSf membrane. However, this result can also be attributed to the increase of the membrane pore sizes which lead to improvement of the water flux. Generally, the improvement of membrane performance was produced by the improvement of the hydrophilicity of the modified PSf membrane which enhanced the water flux, wettability of membrane surface. These observations indicated improved fouling resistance of PSf membrane as the main factor for industrial applications. The modified PSf membrane also is more favorable for salt rejection and various kinds of filtration due to the better properties in terms of permeability, rejection capability and porosity.
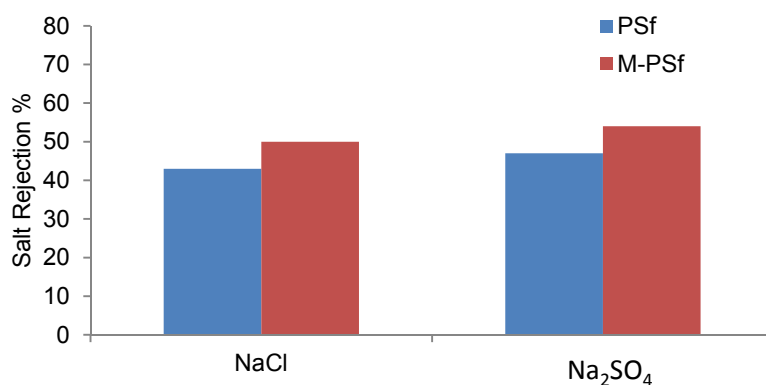

Figure 5: Salt rejection performance of the PSf and modified PSf membranes

4. Conclusion

A α-Fe$_2$O$_3$ NPs with spherical shape were synthesised by the sol gel method using iron nitrate and oxalic acid. The prepared NPs at low concentration (0.50 wt%) were then used to form hybrid PSf membrane by blending. The pure PSf and modified membrane by NPs were characterised and compared. The modified membrane by α-Fe$_2$O$_3$ NPs showed better properties for hydrophilicity, water flux and salt rejection property compared to

pure PSf membrane. It has been observed that the presence of NPs affected the membrane performance. The result form this work indicated that α-Fe$_2$O$_3$ NPs are good additive to improve the ultrafiltration membrane performance.

Acknowledgment

References

Ba-Abbad M.M., Kadhum A.A.H., Mohamad A.B., Takriff M.S., Sopian K., 2012, Synthesis and catalytic activity of TiO2 nanoparticles for photochemical oxidation of concentrated chlorophenols under direct solar radiation, Int. J. Electrochem. Sci. 7, 4871-4888.

Ba-Abbad M.M., Kadhum A.A.H., Mohamad A.B., Takriff M.S., Sopian K., 2013a, Optimization of process parameters using D-optimal design for synthesis of ZnO nanoparticles via sol–gel technique, J. Ind. Eng. Chem. 19, 99-105.

Ba-Abbad M.M., Kadhum A.A.H., Mohamad A.B., Takriff M.S., Sopian K., 2013b, The effect of process parameters on the size of ZnO nanoparticles synthesized via the sol–gel technique, J. Alloys Compd. 550, 63-70.

Ba-Abbad M.M., Kadhum A.A. H., Mohamad A.B., Takriff M.S., Sopian K., 2013c, Visible light photocatalytic activity of Fe 3+-doped ZnO nanoparticle prepared via sol–gel technique, Chemosphere 91,1604-1611.

Ba-Abbad M.M., Chai P.V., Takriff M.S., Benamor A., Mohammad A.W., 2015, Optimization of nickel oxide nanoparticle synthesis through the sol–gel method using Box–Behnken design, Mater. Des 86, 948-956.

Ba-Abbad M.M., Takriff M.S., Mohammad A.W., 2016a, Enhancement of 2-chlorophenol photocatalytic degradation in the presence Co2+-doped ZnO nanoparticles under direct solar radiation, Res. Chem. Intermed. 42, 5219-5236.

Boussu K., Vandecasteele C., Van der Bruggen B., 2006, Study of the characteristics and the performance of self-made nanoporous polyethersulfone membranes. Polymer 47, 3464-3476.

Chung Y.T., Ba-Abbad M.M., Mohammad A.W., Benamor A., 2016, Functionalization of zinc oxide (ZnO) nanoparticles and its effects on polysulfone-ZnO membranes, Desalin. Water Treatment 57, 7801-7811.

Chung Y.T., Ba-Abbad M.M., Mohammad A.W, Hairom N.H.H., Benamor A, 2015, Synthesis of minimal-size ZnO nanoparticles through sol–gel method: Taguchi design optimisation, Mater. Des. 87, 780-787.

Luo M.-L., Zhao J.-Q., Tang W., Pu C.-S., 2005, Hydrophilic modification of poly (ether sulfone) ultrafiltration membrane surface by self-assembly of TiO2 nanoparticles, Appl. Surf. Sci. 249, 76-84.

Mahmoudi E., Ng L.Y., Ba-Abbad M.M., Mohammad A.W., 2015, Novel nanohybrid polysulfone membrane embedded with silver nanoparticles on graphene oxide nanoplates, Chem. Eng. J. 277, 1-10.

Vatanpour V., Madaeni S.S., Moradian R., Zinadini S., Astinchap B., 2011, Fabrication and characterization of novel antifouling nanofiltration membrane prepared from oxidized multiwalled carbon nanotube/polyethersulfone nanocomposite, J. Membr. Sci. 375, 284-294.